IOPscience iopscience.iop.org

Home Search Collections Journals About Contact us My IOPscience

Properties of doped *ex* and *in situ* MgB_2 multi-filament superconductors

This article has been downloaded from IOPscience. Please scroll down to see the full text article.

2006 Supercond. Sci. Technol. 19 1076

(http://iopscience.iop.org/0953-2048/19/10/016)

View the table of contents for this issue, or go to the journal homepage for more

Download details:
IP Address: 130.89.112.86
The article was downloaded on 23/11/2010 at 08:53

Please note that terms and conditions apply.

INSTITUTE OF PHYSICS PUBLISHING SUPERCONDUCTOR SCIENCE AND TECHNOLOGY
Supercond. Sci. Technol. **19** (2006) 1076–1082 doi:10.1088/0953-2048/19/10/016

Properties of doped *ex* and *in situ* MgB_2 multi-filament superconductors

P Kováč[1,4], I Hušek[1], T Melišek[1], E Martínez[2] and M Dhalle[3]

[1] Institute of Electrical Engineering, Centre of Excellence CENG, Slovak Academy of Sciences, Dúbravska cesta 9, 841 04 Bratislava, Slovakia
[2] Instituto de Ciencia de Materiales de Aragón, CSIC—Universidad de Zaragoza, C/María de Luna 3, 50018 Zaragoza, Spain
[3] Department of Applied Physics, Low Temperature Division, University of Twente, PO Box 217, 7500 AE Enschede, The Netherlands

E-mail: Pavol.Kovac@savba.sk

Received 20 July 2006, in final form 28 August 2006
Published 13 September 2006
Online at stacks.iop.org/SUST/19/1076

Abstract
Four-filament *ex* and *in situ* MgB_2 wires were prepared with the rectangular wire-in-tube (RWIT) technique. Based on experience with single-core wires, 10 wt% of W was added to the *ex situ* and 10 wt% of SiC to the *in situ* powders, which were packed into Fe and Nb/AgMg tubes, respectively, and two-axially rolled into composite conductors. The *ex* and *in situ* conductors are compared in terms of field-dependent transport critical current density, effects of filament size reduction and twisting, mechanical behaviour and thermal stability.

(Some figures in this article are in colour only in the electronic version)

1. Introduction

Composite MgB_2 wires made with *in situ* (using a Mg + B mixture) and *ex situ* (using pre-reacted MgB_2) powder-in-tube (PIT) techniques are intensively studied [1–5]. The *ex situ* process requires a final heat treatment at a temperature close to 950 °C to allow recrystallization and sintering of the MgB_2 core, which improves the grain connections substantially [2, 4]. The heat treatment of *in situ* wires requires much lower temperatures (600–750 °C) [5, 6], provoking a solid state or solid–liquid reaction between magnesium and boron. The critical temperature (T_c) and critical current density (J_c) are sensitively influenced by the applied deformation, sheath material and heat treatment conditions [4, 7]. Fe, Ni and Fe-alloy matrices [8–11] lead to the creation of interface layers due to chemical reactions of iron and nickel with boron, which degrade the wire properties. Niobium and tantalum sheaths have been also applied in order to avoid chemical reactions with boron or magnesium [12–15]. Doping of MgB_2 is a promising way to enhance the critical current density in magnetic field of *in situ* [16–20] and possibly also of *ex situ* wires [21]. Up to now, the best $J_c(\mu_0 H)$ performance has been obtained by adding SiC to *in situ* MgB_2 [18–20]. In *ex situ* wires, several metallic powders (Nb, Ti, Zr, Hf and W) were shown to improve the current carrying capacity [21].

SiC particles are decomposed during the final heat treatment and a substitution of boron by carbon increases the upper critical field, which improves J_c in high magnetic fields [19, 20]. Silicon is reacting with Mg and Mg_2Si and Mg_2SiO_4 are the major segregated phases protecting coarse grain structure of MgB_2 [20]. The refined grain structure and nano-size impurities distributed inside the superconducting core can act as effective pinning centres. The presence of tungsten particles influences both the resistivity and also the thermal conductivity of the MgB_2 core, and the improved internal stability is responsible for increased critical current values especially in the low field region [21]. The slope of the $J_c(\mu_0 H)$ dependence has not been changed by adding W or other reactive metals. But, reactive metal additions are beneficial because they preferentially absorb deleterious impurities from the superconducting matrix.

The aim of this work is to present and compare the basic properties of four-filament wires with the most promising additions: W addition to *ex situ* powder and *in situ* precursors with SiC.

[4] Author to whom any correspondence should be addressed.

 © 2006 IOP Publishing Ltd Printed in the UK

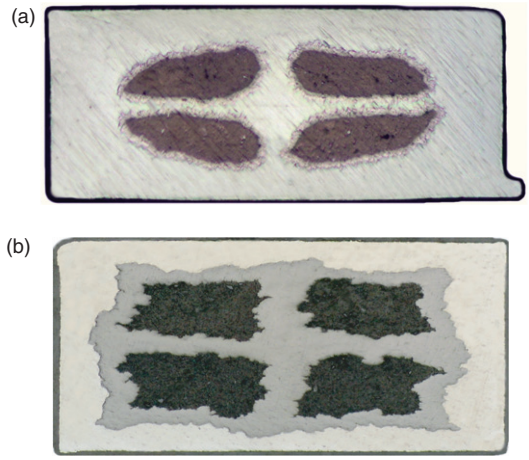

Figure 1. The transversal cross section (a) of four-core EF wire (MgB_2 + 10% W/Fe) 0.56 × 1.23 mm^2 and (b) of IF wire (MgB_2 + 10% SiC/Nb/AgMg) 0.66 × 1.38 mm^2.

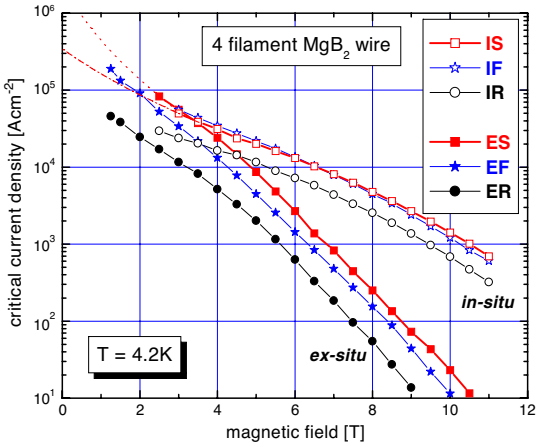

Figure 2. $J_c(\mu_0 H)$ dependence for *ex situ* and *in situ* wires at liquid helium temperature (E—*ex situ*, I—*in situ*, S—square shape, F—flat, R—round).

Table 1. The basic properties of the four-core *ex situ* and *in situ* wires (E—*ex situ*, I—*in situ*, S—square shape, F—flat, R—round).

Wire	Size (mm)	Filaments	Sheath	Heat treatment
ES	1.0 × 1.0	MgB_2–10% W	Fe	950 °C/0.5 h
EF	0.56 × 1.23	MgB_2–10% W	Fe	950 °C/0.5 h
ER	0.83	MgB_2–10% W	Fe	950 °C/0.5 h
IS	1.2 × 1.2	MgB_2–10% SiC	Nb/AgMg	650 °C/0.5 h
IF	0.66 × 1.38	MgB_2–10% SiC	Nb/AgMg	650 °C/0.5 h
IR	1.1	MgB_2–10% SiC	Nb/AgMg	650 °C/0.5 h

2. Experimental details

Commercial MgB_2 powder (particle size 0.1–60 μm) from *Alfa Aesar* was mixed with 10 wt% of W (∼1 μm powder) and homogenized by ball milling for 10 min. After deformation of a single-core wire with Fe matrix, a four-filament composite was assembled into a new Fe tube and further deformed with the rectangular wire-in-tube technique (RWIT) [22]. The re-stacked conductor was two-axially rolled (TAR) into square wires with a 1 × 1 mm^2 cross-section (ES) or into flat conductors with section 0.56 × 1.23 mm^2 (EF). Round four-filament wires (ER) were prepared by cold-drawing a square 1.3 × 1.3 mm^2 wire down to a circular diameter of 0.83 mm. All *ex situ* conductors were given a final heat treatment in argon at 950 °C for 30 min.

Four-filament *in situ* wires were prepared using the same deformation techniques, starting from *Alfa Aesar* Mg (99% purity, ∼20 μm particle size) and B (90%, ∼1 μm) powders mixed with 10 wt% of SiC nano-particles (20 nm). Nb and AgMg alloys were used as inner and outer sheaths, respectively. Square 1.2 × 1.2 mm^2 wires (IS) and flat 0.66 × 1.38 mm^2 conductors (IF) were made by TAR and round wires (IR) with diameter 1.1 mm by drawing. The final reaction was performed in argon at 650 °C for 30 min. Table 1 summarizes the lay-out and heat treatment of all four-core samples, while figure 1 shows the cross-sections of the EF and IF samples.

Longer pieces of the as-deformed EF and IF conductors were wound on a ceramic former of 38 mm diameter into single-layer helical coils, heat-treated as described above and transferred onto a metal frame with current terminals. Transport critical currents (I_c) were measured at 4.2 K in variable external magnetic field using the standard electric field criterion of 1 μV cm^{-1}. The potential taps were separated 5 mm apart for the short (∼5 cm) straight samples and 50 cm apart for the coiled (∼1 m long) samples. Prior to heat-treatment, pieces of the as-deformed square wires ES and IS were twisted with variable pitch to determine the effect of twisting on the critical current.

Quench propagation experiments and self-field I_c measurements were done on 10 cm long pieces of the ES and IS wires, as explained in [23]. The samples were mounted in a cryocooler with the current contacts thermally anchored to the second stage of the cold head. The measurements were made in vacuum at different temperatures, ranging from 15 to 36 K, using a Lakeshore 331 temperature controller. The temperature dependence of I_c was measured using triangular current pulses (duration 1 s). For quench propagation experiments, the voltage development and temperature along the conductor were monitored by a Data Acquisition (DAQ) device. The temperature profile was recorded with K-type thermocouples, which were soldered to the sample to minimize the thermal contact resistance, using the cold finger as the reference temperature. In order to prevent damaging the conductor during a quench, the current was turned off 0.3–2.0 s (depending on the current level and matrix composition) after injecting the energy pulse.

Short heat-treated EF and IF conductors were also bent at room temperature to diameters of 100 and 40 mm to assess the resulting I_c degradation. Pieces of the square ES and IS wires were soldered on a U-shaped spring, with which samples can be stretched or compressed homogeneously in the axial direction [24]. The critical current of these wires was then measured under variable axial tension and compression at 4.2 and 20 K.

3. Results and discussion

3.1. Critical current densities

Figure 2 compares the $J_c(\mu_0 H)$ characteristics at 4.2 K of the *ex situ* wires with 10 wt% of W addition with those of the *in situ*

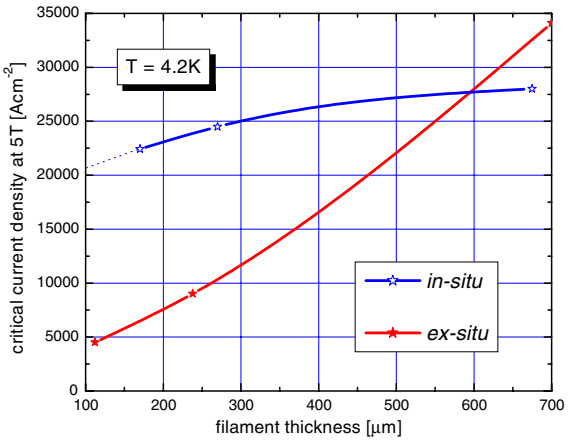

Figure 3. The effect of reduced filament size (between 700 and 100 μm) on the J_c (5 T) of *ex situ* and *in situ* wire.

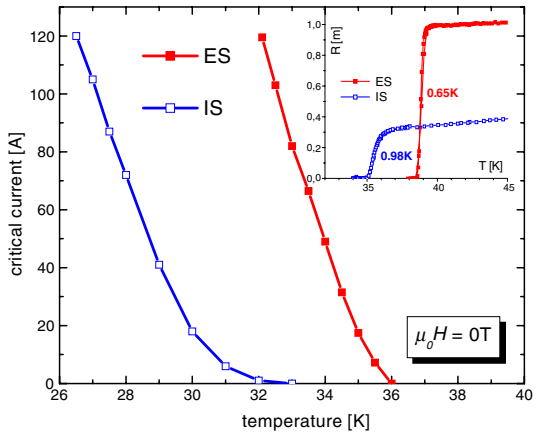

Figure 4. Self-field current densities measured by current pulses at temperatures above 26 K for ES and IS wires. The inset shows the $R(T)$ dependences of both wires.

four-core wires with 10 wt% of SiC. Comparable J_c values are measured for the ES and IS wires only at $\mu_0 H = 3$ T. While the current density of the *ex situ* wires decreases rapidly with external magnetic field (by five orders of magnitude from 0 to 10 T), the J_c of *in situ* wires decays less in the same field range (less than three orders of magnitude). This $J_c(\mu_0 H)$ difference is attributed to the effect of SiC addition to MgB_2, leading to grain size refinement [20] and artificial pinning centres [18].

The highest J_c values were measured for the square wires ES and IS. The effect of flattening is not the same for *ex situ* and *in situ*. The J_c values of EF are about half those of ES, while they are virtually unchanged in the *in situ* wires IF and IS. A similar observation can be made for the drawing into round wires: comparing ER with ES, J_c is reduced by a factor of four to five, but only by a factor $\sim$2 between IR and IS. The dependence of the critical current density on filament size is plotted in figure 3, which shows J_c (5 T, 4.2 K) for filament sizes ranging from 100 to 700 μm. J_c decreases much faster for smaller filaments in the *ex situ* wires. The ratio $J_c(700\ \mu\text{m})/J_c(100\ \mu\text{m})$ is 8.4 for *ex situ*, but only 1.36 for *in situ* wires. This correlates well with the previously discussed effects of wire flattening (filament size reduction) and drawing (filament size and density reduction). Also, the micro-hardness evolution with total area reduction is steeper for *ex situ* than for *in situ* conductors [25]. In *in situ* conductors, the Mg–B core is much softer than the metallic matrix and this hardness difference is measured to remain constant during progressive area reduction. Therefore, the deformation of *in situ* filaments is easier and allows us to obtain smaller filament size without the extensive crack generation that is observed in *ex situ* wires. The J_c degradation with area reduction for *ex situ* wires is found to be due to transversal cracks (the particles in the *Alfa Aesar* MgB_2 powder are hard and have a non-uniform size distribution ranging from 0.1 to 60 μm) [15, 25]. In *ex situ* filaments, where no free elements are available for a new MgB_2 phase formation, these cracks cannot be healed with the final sintering treatment at 950 °C/30 min. On the other hand, the much smaller cracks in the softer Mg–B filaments heal well during heat treatment, due to the Mg–B reaction and MgB_2 phase creation. Therefore, transport J_c values of *in situ* wires are less sensitive to filament size.

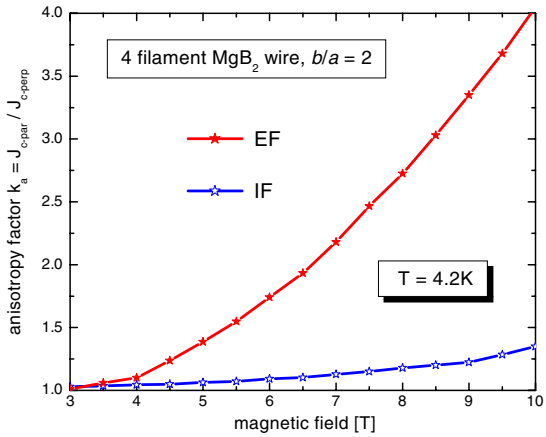

Figure 5. J_c anisotropy of EF and IF samples having the same aspect ratio $b/a = 2$ measured at 4.2 K.

The high self-field transport J_c values cannot be measured at 4.2 K due to poor thermal stability. Only a rough extrapolation of J_c (0 T, 4.2 K) is made in figure 2, yielding current densities above 3×10^5 A cm^{-2} for the IS wire and above 2×10^6 A cm^{-2} for the ES one. Figure 4 shows the self-field critical current of the ES and IS wires, measured using short triangular current pulses at temperatures above 26 K. These high-temperature data confirm the higher J_c (0 T) for *ex situ* wire. The inset in figure 4 shows the $R(T)$ transition, with a more than 3 K higher T_c value and a narrower transition for the ES wire. These differences originate in the lower annealing temperature used for the *in situ* process and also in the SiC addition that reduces the critical temperature [20]. On the other hand, the Nb/AgMg-sheathed IS wire has a lower normal state resistance.

It is well known that flattening of both *ex situ* and *in situ* filaments leads to grain alignment (texture) and consequently to J_c anisotropy for variable external field orientation [26–28]. Figure 5 shows the anisotropy of J_c at 4.2 K (expressed by the factor $k_a = J_{c-par}/J_{c-perp}$) for EF and IF wires. It is evident that the anisotropy of *ex situ* wire is a few times larger than that of the *in situ* wire with the same aspect ratio (width/thickness) $b/a = 2$. At 10 T, k_a is about three times

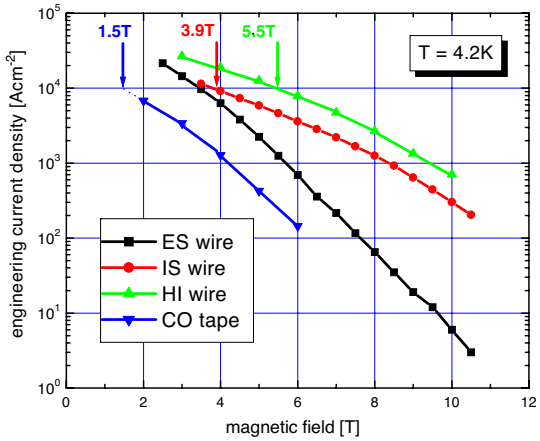

Figure 6. Engineering current density J_e of ES and IS compared with commercial wires CO (Columbus) and HT (Hyper Tech).

larger for the EF wire than for the IF one. This is partly explained by the stronger Fe sheath used for the EF conductor, compared to the Nb/AgMg matrix of the IF wire. As a result, the MgB_2/Fe interface is much smoother than the MgB_2/Nb interface. In addition, the SiC particles (artificial pinning centres) depress the effect of texture on the final $J_c(\mu_0 H)$ characteristic [28]. It should be noted that a lower anisotropy can be advantageous for magnet windings operated at elevated temperature (around 20 K), where the total magnet current can be reduced substantially by radial magnetic field components.

The engineering current densities of the ES and IS wires are compared with those of MgB_2 wires commercially produced by Columbus Superconductors (CO) and Hyper Tech Research (HI). Figure 6 presents $J_e(\mu_0 H)$ data for the four-filament ES (1.00 mm^2) and IS (1.44 mm^2) wires, a 14-filament CO tape (2.34 mm^2) [29] and an 18-filament HI circular wire (0.64 mm^2) [30], all measured at 4.2 K. Similar slopes of J_e versus $\mu_0 H$ are evident for both *ex situ* conductors (ES and CO) and also for the *in situ* wires with SiC addition (IS and HI). Of course, the relative cross-sectional areas of filaments and matrix (fill factors) are different: ES $= 25\%$, IS $= 26\%$, CO $\approx 11\%$ and HI $\approx 19\%$, which influences the engineering current density substantially.

3.2. Twisting effect

The effect of twisting on the $I_c(\mu_0 H)$ characteristic of the IS wire is shown in figure 7(a). At high magnetic field ($\mu_0 H > 7.5$ T) the critical current is hardly influenced, but for lower fields (3.5–7.0 T) I_c degradation becomes significant. Similar behaviour is measured for the ES wire. The reason for this larger I_c degradation in the low field region is not yet understood. Figure 7(b) shows the normalized critical currents of the ES and IS wires at 5 and 9 T versus the ratio of twist pitch to wire size L_t/a ($a = 1$ mm for wire ES, 1.2 mm for IS). No I_c degradation is observed for $L_t/a > 100$. At twist pitches $L_t/a < 75$, the critical current starts to degrade sharply and at 5 T only 40% of the original I_c value is measured for the ES wire twisted to $L_t/a = 40$. In general, the I_c degradation in the ES wire is nearly twice as important as in the IS one. Just like the higher sensitivity to filament area reduction (figure 3),

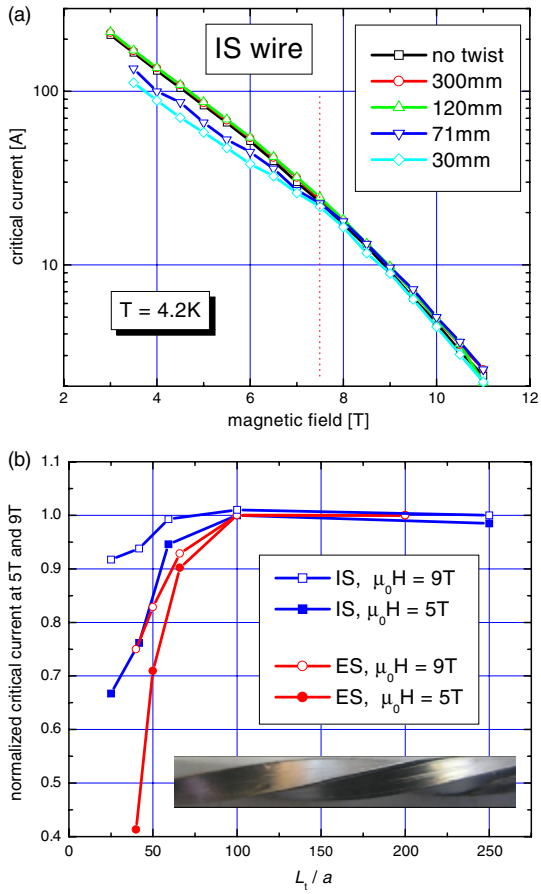

Figure 7. The effect of twisting applied for IS wire, (a) $I_c(\mu_0 H)$ characteristics at variable twist pitches, (b) normalized critical currents versus the twist pitch to wire size (L_t/a) ratio.

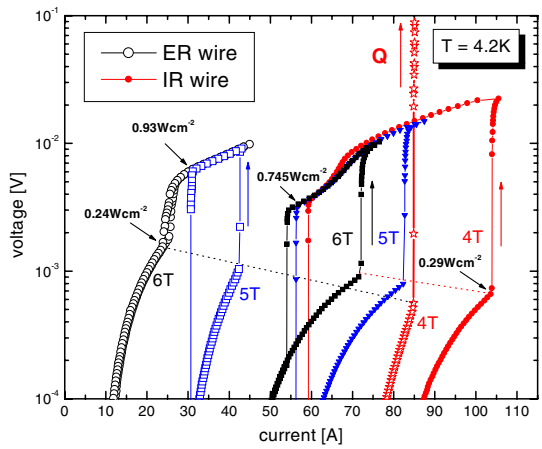

Figure 8. Current–voltage characteristics of ES (open symbols) and IS wires (closed symbols) measured above the level of critical current in the voltage range 10^{-4}–10^{-1} V at $T = 4.2$ K and $\mu_0 H = 4$, 5 and 6 T. The voltage tap separation was 0.5 cm.

this is attributed to the different crack-healing mechanisms in the *ex* and *in situ* processes.

3.3. Wire stability

Figure 8 shows current–voltage characteristics of wires ES and IS, measured well above the electric field criterion for

increasing and decreasing currents at 4.2 K and variable external fields. The transport current is still distributed between the MgB_2 filaments and the metallic sheath in the voltage range 10^{-4}–10^{-3} V. A sudden transition (quench) into the metallic sheath is observed around 10^{-3} V. The precise voltage level at which this transition occurs decreases with increasing current (corresponding to a constant power $I \times V$ or heat generation). Dotted lines show the corresponding constant power densities for both wires, calculated as power per sample surface area, which are not the same for the ES (≈0.24 W cm^{-2}) and IS wires (≈0.29 W cm^{-2}) and correspond to the helium film/bubble boiling transition. The higher power density in the IS wire reflects its better thermal stability. While irreversible quenching occurs at 84.8 A for the ES wire, it was possible to measure the IV characteristic of the IS wire reversibly up to 104 A. Figure 8 also shows that the power densities at which current starts to flow again inside the MgB_2 filaments are also different (<0.93 W cm^{-2} for the ES wire and ≈0.745 W cm^{-2} in the IS one). This difference is not yet understood, but may also be influenced by variable grain connectivity of *ex situ* and *in situ* filaments. Summarizing, the IV characteristics confirm the better thermal stability of the IS wire with the higher conductivity Nb/AgMg matrix.

Normal-zone development and propagation for point disturbance experiments were also carried out to analyse the thermal stability of these same wires. The measurements were made at self-field and under adiabatic conditions, as explained in [23]. Heat pulses were applied to the conductors at $t = 0$, with a typical duration of 5–20 ms. The minimum energy needed to trigger a quench corresponds to the minimum quench energy, MQE. Figure 9(a) shows the time evolution of the electric field along the ES and IS wires during a quench, at $T_0 = 20$ K and $I_t = 100$ A. The different resistivities of both wires, shown in the inset of figure 4 and also observed in these measurements, clearly influence the normal-zone development. In the ES wire, the electric field increases suddenly to the normal-state value $E = E(T_c)$, which is reached already at $t \approx 0.03$ s; for the IS wire, current sharing is observed up to $t \approx 0.16$ s. The transition is also more gradual: an electric field of ∼2 m V cm^{-1} persists for 0.1 s before becoming unstable and increasing to $E(T_c)$. Accordingly, the temperature increase during a quench is faster in the ES wire, as shown in the inset of figure 9(a).

The better thermal stability of IS wire, with a lower resistance Nb/AgMg sheath compared to Fe for the ES wire, is also reflected in the MQE values. The temperature dependence of the experimentally estimated MQE for the ES and IS samples at a transport current $I_t = 100$ A is shown in figure 9(b). MQE values are higher for sample IS, although due to the lower T_c of this sample, both curves will cross over at $T = 27.6$ K. On the other hand, the normal zone propagation velocity $v_p(T_0)$ is systematically lower for sample IS. Although this difference in v_p is not completely understood, it is believed to be related to the bigger cross section and the smoother I–V transitions of the IS wire (figure 8).

3.4. Wind-and-react coils and mechanical effects

Room-temperature bending of the EF and IF conductors causes critical current degradation. Compared to straight samples, I_c (5 T, 4.2 K) of EF and IF degrades to 33–46% of the original current for bending diameter 100 mm and to only ∼20% for 40 mm. Therefore, single-layer helical coils of 38 mm diameter were made from EF and IF wires with the 'wind-and-react' technique; see figure 10. Compared to straight short sample data, the critical current measurements of the EF coil show no I_c degradation, while close to 10% I_c degradation was estimated for the IF coil. The partial degradation of the IF wire is likely due to the handling of the coil during transfer from the ceramic heat-treatment former to the metallic barrel with current terminals. The mechanical strength of annealed Nb/AgMg is lower than that of iron, rendering the EF wire more robust. Furthermore, generally a more brittle behaviour is observed for *in situ* MgB_2 conductors compared to *ex situ* ones [31].

Figure 11 shows the normalized critical currents of the ES and IS wires exposed to axial compressive and tensile strain. The characteristics were measured at different temperatures and magnetic fields, which may influence the slope of the $I_c(\varepsilon)$ dependence but not the irreversible strains ε_{irr} [24]. Values

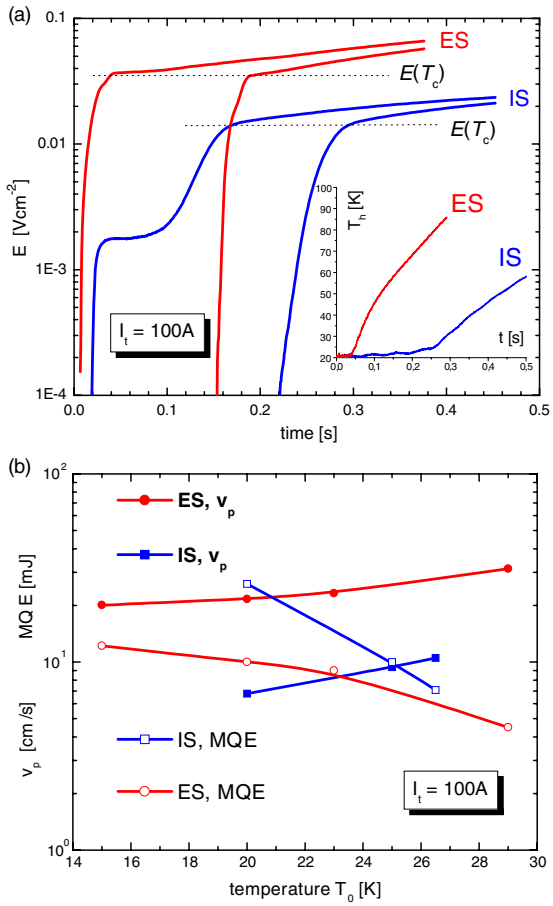

Figure 9. (a) Time evolution of the electric field along the ES and IS wires during a quench at $T_0 = 20$ K and $I_t = 100$ A. The distance between both voltage taps was 3.3 and 0.9 cm for ES and IS, respectively. Thick lines correspond to $E(t)$ measured around the heater. The dotted lines mark the E value at $T = T_c$ for each sample. Inset, temperature evolution of the hot point for the same wires and conditions. (b) Minimum quench energies, MQEs, and quench propagation velocities, v_p, of ES and IS wires as a function of temperature for constant transport current 100 A.

Figure 10. Single-layer helical coils wound of EF and IF wires on the ceramic former of 38 mm diameter and connected to current terminals.

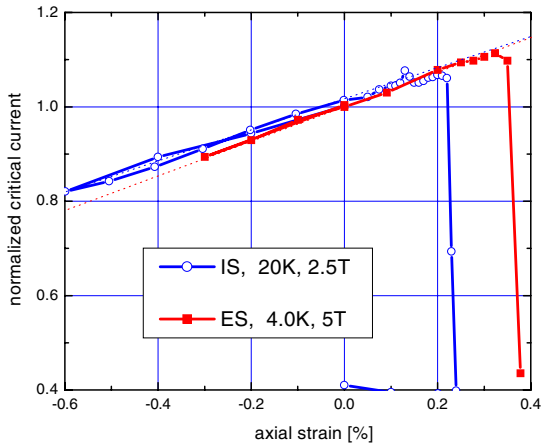

Figure 11. The normalized critical current versus axial strain obtained for ES wire at 4.2 K and 5 T and for IS wire at 20 K and 2.5 T.

of $\varepsilon_{irr} = 0.2\%$ and 0.33% are obtained for wires IS and ES, respectively. The higher sensitivity of the IS wire to mechanical strain correlates well with the partial I_c degradation of the coil sample wound from the IF conductor and also with previously published data showing different tensile strain degradations for *ex* and *in situ* single-core wires [31]. The higher filament porosity resulting from the diffusion/reaction in the *in situ* process is the main reason for this more brittle behaviour.

4. Conclusions

Transport current characteristics of doped *ex situ* MgB_2/Fe and *in situ* MgB_2/Nb/AgMg four-filament wires were studied and compared. While at 4.2 K the current density of *ex situ* wires with W addition decreases by five orders of magnitude in the external magnetic field range from 0 to 10 T, the J_c of *in situ* wires with SiC decreases by less than three orders in the same range. J_c decrease with filament size reduction is much more serious for *ex situ* wires. Cracks induced during composite deformation are more effectively healed during *in situ* reaction than in *ex situ* sintering.

Similarly, for twist pitches below ~75 mm nearly twice as high an I_c degradation by twisting was observed for *ex situ* wire compared to *in situ*. This is also attributed to cracks induced by torsion deformation, which cannot be healed sufficiently by heat treatment of *ex situ* filaments. Tensile irreversible strains at 4.2 K of $\varepsilon_{irr} = 0.2\%$ and 0.33% are measured for *in situ* and *ex situ* wires, respectively.

IV characteristics and quench measurements confirm the improvement of thermal stability of the *in situ* wire, having a lower-resistance and better thermal conductivity Nb/AgMg sheath, compared to the higher-resistance Fe-sheathed *ex situ* wire.

Acknowledgments

This work was supported by the Science and Technology Assistance Agency under the contract number APVT-51-029902, and by the EU FP6 contract number NMP3-CT2004-505724. Authors would like to thank T Holúbek for the *I–V* characteristic measurements.

References

[1] Zhao Y, Feng Y, Cheng C H, Zhou L, Wu Y, Machi T, Fudamoto Y, Koshizura N and Murakami M 2001 *Appl. Phys. Lett.* **79** 1154
[2] Suo H L, Beneduce C, Dhallé M, Musolino N, Genoud J E and Flükiger R 2001 *Appl. Phys. Lett.* **79** 3116
[3] Cimberle M R, Novak P, Manfrinetti P and Palenzona A 2002 *Supercond. Sci. Technol.* **15** 43
[4] Kováč P, Hušek I and Melišek T 2002 *Supercond. Sci. Technol.* **15** 1340
[5] Dou X, Horvath J, Soltanian S, Wang X L, Qin M J, Zhou S H, Liu H K and Munroe P G 2003 *IEEE Trans. Appl. Supercond.* **13** 3199
[6] Fu B Q, Feng Y, Yang G, Liu C F, Zhou L, Cao L Z, Ruan K Q and Li X G 2003 *Physica* C **392–396** 1035
[7] Kováč P, Hušek I, Melišek T and Štrbík V 2005 *Supercond. Sci. Technol.* **18** 856
[8] Pachla W, Presz A, Kováč P, Hušek I and Diduszko R 2004 *Supercond. Sci. Technol.* **17** 1289
[9] Grasso G, Malagoli A, Ferdeghini C, Roncallo S, Braccini V, Cimberle M R and Siri A S 2001 *Appl. Phys. Lett.* **79** 230
[10] Yamamoto A, Shimojama J, Ueda S, Katsura Y, Horii S and Kishio K 2004 *Supercond. Sci. Technol.* **17** 921
[11] Kumakura H, Matsumoto A, Fujii H and Togano K 2001 *Appl. Phys. Lett.* **79** 2435
[12] Goldacker W, Schlachter S I, Zimmer C and Reiner H 2001 *Supercond. Sci. Technol.* **14** 787
[13] Feng Y, Yan G, Zhao Y, Liu C F, Fu B Q, Zhou L, Cao L Z, Ruan K Q, Li X G, Shi L and Zhang Y H 2003 *Physica* C **386** 598
[14] Fu B Q, Feng Y, Yan G, Liu C F, Zhou L, Cao L Z, Ruan K Q and Li X G 2003 *Physica* C **392** 1035

[15] Kováč P, Hušek I, Melišek T, Kulich M and Štrbík V 2006 *Supercond. Sci. Technol.* **19** 600
[16] Zhao Y, Feng Y, Cheng C H, Zhou L, Wu Y, Machi T, Fudamoto Y, Koshizura N and Murakami M 2001 *Appl. Phys. Lett.* **79** 1145
[17] Ma Y, Kumakura H, Matsumoto A and Togano K 2003 *Appl. Phys. Lett.* **83** 1181
[18] Dou X, Horvath J, Soltanian S, Wang X L, Qin M J, Zhou S H, Liu H K and Munroe P G 2003 *IEEE Trans. Appl. Supercond.* **13** 3199
[19] Sumption M D, Bhatia M, Ridfleisch M, Tomsic M, Soltanian S, Dou S X and Collings E W 2005 *Appl. Phys. Lett.* **86** 092507
[20] Pachla W, Morawski A, Kováč P, Hušek I, Mazur A, Lada T, Diduszko R, Melišek T, Štrbík V and Kulczyk V 2006 *Supercond. Sci. Technol.* **19** 1
[21] Kováč P, Hušek I, Melišek T, Grovenor C R M, Haigh S and Jones H 2004 *Supercond. Sci. Technol.* **17** 1225
[22] Kováč P, Hušek I, Melišek T, Dhallé M, Müller M and den Ouden A 2005 *Supercond. Sci. Technol.* **18** 615
[23] Martínez E, Lera F, Martínez-López M, Schlachter S I, Lezza P and Kovác P 2006 *Supercond. Sci. Technol.* **19** 143
[24] Dhallé M, van Weeren H, Wessel S, den Ouden A, ten Kate H, Hušek I, Kováč P, Schlachter S and Goldacker W 2005 *Supercond. Sci. Technol.* **18** S253
[25] Kováč P, Hušek I and Melišek T 2006 *CIMTEC'06 Conf. (Acireale, June 2006)*
[26] Kumakura H, Matsumoto A, Fujii H, Kitaguchi H and Togano K 2002 *Physica* C **382** 93
[27] Lezza P, Gladyshevskii R, Senatore C, Cusanelli G and Flükiger R 2005 *IEEE Trans. Appl. Supercond.* **15** 3196
[28] Kováč P, Melišek T and Hušek I 2005 *Supercond. Sci. Technol.* **18** L45
[29] Kitagushi H and Kumakura H 2005 *Supercond. Sci. Technol.* **18** S284
[30] Tomsic M, Rindfleish M, Yue J, McFadden K, Peng X and Doll D 2005 *Poster presented at the EUCAS-Conf. (Sept. 2005)*
[31] Kováč P, Melišek T, Dhallé M, den Ouden A and Hušek I 2005 *Supercond. Sci. Technol.* **18** 1374